Article:
Jiang, L, Wang, H, Gao, C et al. (4 more authors) (2022) Skin color measurements before and after two weeks of sun exposure. Vision Research, 192. 107976. p. 107976. ISSN 0042-6989

https://doi.org/10.1016/j.visres.2021.107976

Skin Color Measurements Before and After Two Weeks of Sun Exposure

Li Jiang [a], Han Wang [b], Cheng Gao [b], Xiaohui Zhang [b], Kaida Xiao [c], Manuel Melgosa [d], Changjun Li [b,*]

[a] School of Physical Education, University of Science and Technology Liaoning, Anshan, China
[b] School of Computer and Software Engineering, University of Science and Technology Liaoning, Anshan, China
[c] School of Design, University of Leeds, Leeds, UK
[d] Department of Optics, University of Granada, Granada, Spain
* Corresponding author: Changjun Li, cjliustl@sina.com

ABSTRACT

We performed spectrophotometric measurements of skin reflectance at four body locations (forehead, cheek, neck, and back of hand), before and after two weeks of sun exposure, for 103 first-year college students. Skin reflectance was measured twice at each body location, before and after two weeks of sun exposure, obtaining an average repeatability (mean color difference from the mean) in the range of 0.2-0.5 CIELAB units (D65 illuminant, CIE 1931 standard observer). However, the average skin color differences before and after two weeks of sun exposure were in the range of 3.6-3.9 CIELAB units, considerably higher than measured repeatability, as a consequence of suntanning. Skin color appearance variation was analyzed in the CIELAB color space, and it was found that at all body locations two weeks of sun exposure made lightness L^* and hue-angle h_{ab} significantly decrease, a^* and chroma C^*_{ab} significantly increase, and b^* shows no statistically significant changes (except for h_{ab} at the forehead and cheek, and for a^* at the forehead where no statistically significant changes were found). An W shape for skin spectral reflectance between 520 nm and 600 nm was found at some of the four measured body locations. It was found that the individual typological angle (ITA) defined from L^* and b^* performed well in predicting our measured data and a modification of ITA using L^* and C^*_{ab} performed even better, with the measured L^* as reference. The color shifts produced by two weeks of sun exposure in different planes of CIELAB were analyzed for the skin categories established by the ITA index, and compared with the control group data accumulated by Amano et al. (PLoS ONE. 15(12), e0233816)(PLoS ONE 15(2020) e0233816). The measured skin spectra can be useful to the skin color database currently being developed by CIE TC 1-92.

KEYWORDS

skin reflectance, individual typological angle (ITA), CIELAB color space

1. INTRODUCTION

Human skin color has been the subject of numerous studies, dealing with the measurement and characterization of variations according to ethnicity and body locations (Han, Choi, & Son, 2006; Xiao

et al., 2012; Xiao et al., 2017; Wei et al., 2007), the evaluation of uncertainty in measurements using different instruments (Wang et al., 2018), color measurement for the design and evaluation of cosmetic products (Amano et al., 2020; Melgosa et al., 2018), health care under ultraviolet radiation (Chardon, Cretois, & Hourseau, 1991; Durand et al., 2020), color segmentation for face detection and recognition (Bilal et al., 2015; Brancati et al., 2016; Mendenhall, Nunez, & Martin, 2015), accurate skin color reproductions (Xiao et al., 2013; Xiao et al., 2016), skin optics studies for establishing spectral reflectance models and chromophores (Schmitt & Kumar, 1996; Young, 1997; Zonios et al., 1999; Zonios, Bykowski, & Kollias, 2001), etc. The International Commission on Illumination (CIE) has set up its Technical Committee 1-92 (CIE TC 1-92) to create a skin color database for different industrial applications, and this committee is collecting skin reflectance measurements for different ethnicities, genders, ages and body locations. Currently, we are developing a project to collaborate with CIE TC 1-92 by gathering skin spectral data before and after aerobic and anaerobic exercise. The aim of this project is to obtain new spectral data and to examine the changes in skin color appearance before and after different forms of exercise and their dependency on body location, using the CIELAB color space.

In a previous paper (Jiang et al., 2021) we reported skin color results before and after 100-meter sprinting and found that this sprinting considerably changed the values of the CIELAB red-green a^* coordinate, while the lightness L^* and yellow-blue b^* coordinates remained almost constant. In addition, it was found that the red-green a^* variation depends on body location. On average, a^* decreased after sprinting at the forehead, cheek, and neck locations while the opposite was true at the inner forearm. Note that 100-meter sprinting may be considered as an anaerobic sport exercise. In the current paper, we will report skin spectral reflectances measured for college students before and after two weeks of sun exposure during military training (henceforth designated as TWSE from the initials of "two weeks sun exposure"), which may be considered a period of practice for several aerobic sport exercises. In China, when new students enter university every year, they receive this training before their academic studies begin, at the end of August or in early September. In this period, the weather is very hot and the TWSE course is mainly done outdoors, which implies that the students' faces, necks, cheeks and hands are exposed to natural sunlight. Consequently, during TWSE, the concentration of melanin in the skin increases (Amano et al., 2020; Chardon, Cretois, & Hourseau, 1991; Zonios, Bykowski, & Kollias, 2001), and their skin becomes darker. Hence, the results in the current paper can be considered useful for showing skin color appearance variations after a natural sunlight tanning process.

In addition to providing spectral skin data to CIE TC1-92 for related applications, the motivation behind the current paper is three-fold. First, in addition to the lightness L^* variation in CIELAB space, we want to determine whether the red-green a^*, yellow-blue b^*, chroma C^*_{ab}, and hue-angle h_{ab} have any systematic variations, and whether these variations are dependent on body location. Second, from the measured skin colors we want to evaluate the usefulness of the individual typological angle (ITA) (Chardon, Cretois, & Hourseau, 1991), which was developed to establish the skin categories designated as very light skin (VLS), light skin (LS), intermediate skin (IS) and tan skin (TS), which have been shown to be linearly correlated to melanin concentration by Zonios et al.(Zonios, Bykowski, & Kollias, 2001). Third, we will examine the color shifts in different planes of the CIELAB space, using the skin categories established by the ITA index. In general terms, the present paper focuses on accurately describing the skin color changes produced by TWSE.

Figure 1 Illustration of measured locations at forehead (1), cheek (2), neck (3), and back of hand (4).

2. EXPERIMENT DESIGN

Skin measurements were made using a calibrated Konica Minolta CM-2600d spectrophotometer with d:8° measurement geometry and 8 mm aperture size (Konica Minolta, 2014). Spectral reflectance factors were measured in the range of 360-740 nm (10 nm steps) at four different body locations (forehead, cheek, neck, and back of hand), as shown in Figure 1. From the manufacturer of this spectrophotometer, the standard deviation of measurements performed are below 0.2% for spectral reflectance factors, and within 0.04 CIELAB units for a white calibration plate measured 30 times at 10-second intervals. Our whole measurement procedure obtained the ethical approval from the University of Science and Technology Liaoning Research Ethics Committee.

A total of 103 students from the University of Science and Technology Liaoning (Anshan, China) were recruited for these measurements, which were carried out the day before and the day after the TWSE. At each body location, we performed two consecutive measurements without moving the instrument. We therefore performed a total of 3,296 spectrophotometric measurements [103 students x 4 body locations x 2 time points (before and after TWSE) x 2 replicate measurements x 2 measurement modes (specular component included, SCI, and specular component excluded, SCE)]. While the CM-2600d spectrophotometer measures spectral reflectance factors simultaneously in SCI and SCE modes, for all data analyses in the following sections we employed only the reflectances measured in the SCE mode.

3. MEASURED DATA EVALUATION IN CIELAB SPACE

First, the repeatability of the measurements made with the CM-2600d spectrophotometer was determined. Let $r_{j,k,i}$ represent the measured spectral reflectance factor, where the subindices j, k and i indicate the participant, the body location, and the number of replications, respectively. In this case, initially j=1,…,103, k=1,…,4; i=1,2. We also designated as $Lab_{j,k,i}$ the CIELAB coordinates calculated from $r_{j,k,i}$ under the CIE standard illuminant D65 and the CIE 1931 standard colorimetric observer using the CIE standard procedure (CIE, 2018). CIELAB is one of two approximately uniform color spaces currently recommended by CIE. CIELAB is a Euclidean color space with coordinates L^*, $a^*$and b^*, which has been widely used for color specification of object colors and evaluation of color

differences, as well as a color appearance model (Fairchild, 2013). In this last sense, CIELAB provides correlates of three main perceptual color attributes (lightness, L^*, chroma, C^*_{ab}, and hue-angle, h_{ab}). Experimental results showed that the human visual system can distinguish these three color attributes and is particularly sensitive to hue and lightness (Melgosa et al., 1999, 2000; Zhang & Montag 2006).

Let NS be the number of students participating in the experiment. The average CIELAB coordinates $Lab_{j,k,ave}$ can be computed using Eq. (1):

$$Lab_{j,k,ave} = (Lab_{j,k,1} + Lab_{j,k,2})/2 \ . \quad (1)$$

The color difference $\Delta E_{j,k,i}$ between $Lab_{j,k,i}$ and $Lab_{j,k,ave}$ defined by Eq. (2) below represents the *i*-th measurement variation for the *j*-th participant at the *k*-th body location

$$\Delta E_{j,k,i} = \Delta E(Lab_{j,k,i}, Lab_{j,k,ave}) \ . \quad (2)$$

$\Delta E_{j,k}$ defined by Eq. (3) below represents the measurement repeatability for the *j*-th participant at the *k*-th body location

$$\Delta E_{j,k} = (\Delta E_{j,k,1} + \Delta E_{j,k,2})/2 \ . \quad (3)$$

ΔE_k defined by Eq. (4) below is the so-called mean color difference from the mean, MCDM, and represents measurement repeatability (Wang et al., 2018; Jiang et al., 2021) for the *k*-th body location

$$\Delta E_k = \frac{1}{NS}\sum_{j=1}^{NS} \Delta E_{j,k} \ . \quad (4)$$

Finally, we introduce the subindices *B* and *A* to indicate color measurements performed before and after TWSE, respectively. Thus, $Lab_{A:j,k,ave}$ and $Lab_{B:j,k,ave}$ represent the average CIELAB coordinates for the *j*-th participant at the *k*-th body location after and before TWSE, respectively. Therefore, $\Delta E_{BA:j,k}$ defined by Eq. (5) below represents the CIELAB color difference before and after TWSE for the *j*-th participant at the *k*-th body location

$$\Delta E_{BA:j,k} = \Delta E(Lab_{B:j,k,ave},\ Lab_{A:j,k,ave}). \quad (5)$$

Thus, $\Delta E_{BA:k}$ defined by Eq. (6) below represents the average CIELAB color difference before and after TWSE for the *k*-th body location, which is mainly attributable to natural suntanning

$$\Delta E_{BA:k} = \frac{1}{NS}\sum_{j=1}^{NS} \Delta E_{BA:j,k} \ . \quad (6)$$

Table 1 lists, for each body location (column 1), the number of students (NS) (column 2) after removing outliers. Measurements repeatability for each body location before ($\Delta E_{B:k}$) and after ($\Delta E_{A:k}$) TWSE is listed in columns 3 and 4, respectively. The last column in Table 1 (column 5) shows the average CIELAB color difference ($\Delta E_{BA:k}$) produced by TWSE for each of the four body locations. From Table 1, the repeatability of our measurements ranges from 0.2 CIELAB units for the back of the hand to 0.5 CIELAB units for the forehead and neck locations. However, the average color differences between skin colors before and after TWSE for each body location range from 3.6 to 3.9 CIELAB units, which are well above measurement error (repeatability) as defined in Eq. (4). Therefore, the effect of TWSE, mainly a natural suntanning, on the variation in skin color is considerably high (3.6-3.9 CIELAB units). To understand the magnitude of these color differences we should note that, for human observers with normal color vision, 0.6-1.1 CIELAB units are typical visual threshold values for homogeneous object colors (Huang et al., 2015).

We further evaluated the $\Delta E_{j,k}$ (or more exactly, $\Delta E_{B:j,k}$ and $\Delta E_{A:j,k}$) color differences for a fixed *k*-th body location using the MATLAB function "boxplot". This function considers $\Delta E_{j,k}$ larger than $q_3 + w \times (q_3 - q_1) / \text{sqrt}(n)$ or smaller than $q_1 - w \times (q_3 - q_1) / \text{sqrt}(n)$ as outliers, where q_1 and q_3 are the 25th and 75th percentiles, respectively, of the sample data, *n* is the number of data, and w is a weight

with a default software value of 1.57. Therefore, the outlier data were removed by using this function. If the measured data for the k-th body location for a particular participant was found to be an outlier before/after TWSE, then the corresponding measured data after/before TWSE for the same body location and participant was removed as well. For each body location, this process was repeated until there were no outliers either before or after TWSE.

Body location	NS	$\Delta E_{B:k}$	$\Delta E_{A:k}$	$\Delta E_{BA:k}$
Forehead	94	0.5	0.5	3.9
Cheek	88	0.4	0.3	3.9
Neck	98	0.5	0.5	3.9
Back of hand	87	0.2	0.2	3.6

Table 1 Repeatability of our measurements for different body locations before (column 3) and after (column 4) TWSE, and the average skin color differences (column 5) produced. All values in Table 1 are CIELAB units (D65 standard illuminant, CIE 1931 standard colorimetric observer). NS is the number of students participating in the experiment after removing all outliers.

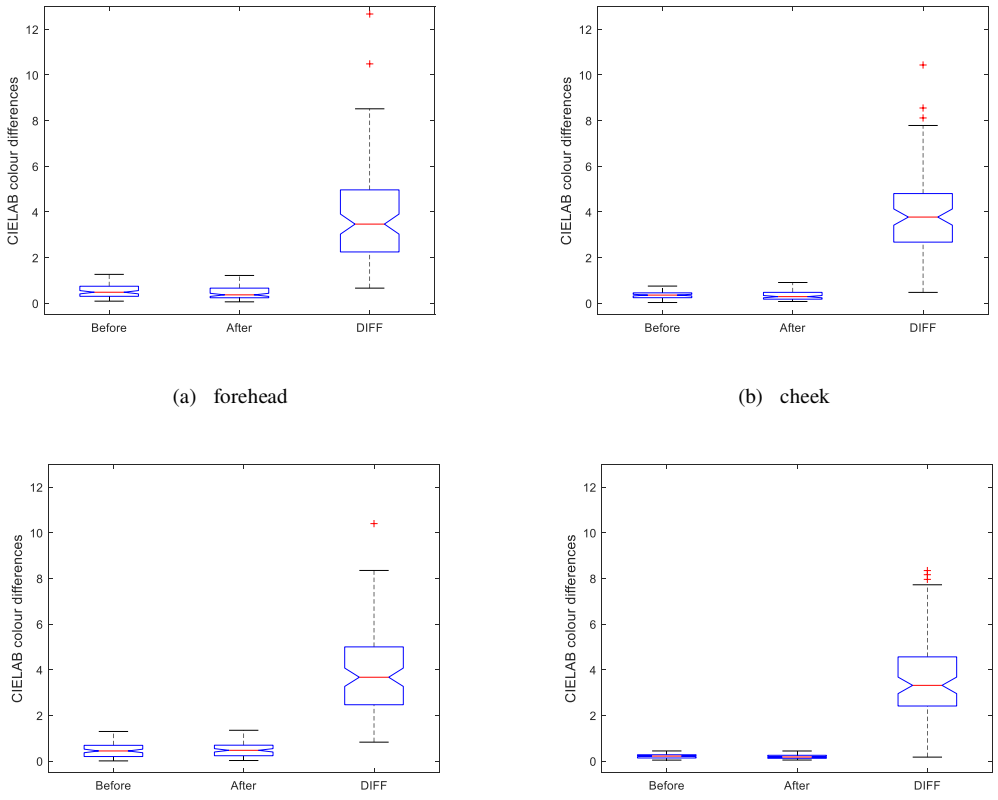

(a) forehead (b) cheek

(c) neck (d) back of hand

Figure 2 CIELAB color differences in our experiment for forehead (a), cheek (b), neck (c), and back of hand (d). For each of the four body locations, the horizontal axes consider the repeatability of measurements "before" and "after" TWSE (see Eq. 4), while "DIFF" indicates skin color differences produced by TWSE (see Eq. 6) or due to natural suntanning. In each box, the central red mark indicates the median, and the bottom and top edges indicate the 25th and 75th percentiles, respectively. The whiskers (short segments above and below the box) extend to the most extreme data points not considered to be outliers, and the outliers are plotted individually using the + symbol.

Figure 2 shows box-plots with notches illustrating the repeatability of our measurements "before" and "after" TWSE, obtained from Eq. 4, as well as the skin color differences produced by TWSE, which are designated "DIFF" and were obtained from Eq. 6, distinguishing the four body locations: forehead (a), cheek (b), neck (c), and back of hand (d). In each of these box-plots, the red mark in the middle of the notch indicates the median, and the bottom and top edges of the box indicate the 25th and 75th percentile CIELAB color differences, respectively, while whiskers (segments above and below the box) extend to the extreme data points not considered to be outliers, and the outliers are plotted individually using the + symbol (see box-plots 3). In Figure 2 there is no outlier for box-plots "before" and "after" TWSE in any of the four diagrams because the outliers were first removed. However, there are still some outliers in box-plot "DIFF" for each of the body locations, which cannot be considered as outliers in our analysis, and show some of the effects of skin color variation produced by TWSE. It can be seen in each of the four diagrams in Fig. 2 that the average values in box-plot "DIFF" are considerably higher than those in box-plots "before" and "after", which means that skin color variation produced by TWSE (Eq. 6) or by two-week natural suntanning is much higher than repeatability of measurements (Eq. 4) in the four body locations. In fact, in each of the four diagrams in Figure 2, the notch for the box-plot "DIFF" does not overlap with the notches in the box-plots "before" and "after". Therefore, according to the help document of the MATLAB function "boxplot", at 95% confidence level the color differences in box-plots "DIFF" (i.e. CIELAB color differences produced by TWSE, computed from Eq. 6) are statistically significantly higher than those in box-plots "before" or "after" (i.e. CIELAB color differences computed from Eq. 4, representative of measurements repeatability before or after TWSE).

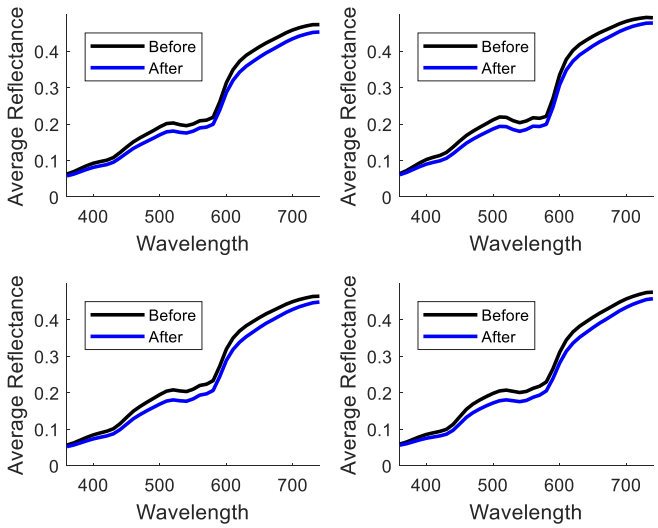

Figure 3 Average spectral reflectance factors of skin before (black) and after (blue) TWSE at 4 body locations: forehead (top left), cheek (top right), neck (lower left), and back of hand (lower right).

Figure 3 shows the average measured spectral reflectance factors of the skin before (black curves) and after (blue curves) TWSE at the four body locations: forehead (top left), cheek (top right), neck (lower left), and back of hand (lower right). It can be noted that for all body locations the black curves are above the blue curves. We can also note that measured skin spectral reflectances have a characteristic W shape between 520 nm and 600 nm, with a magnitude dependent on body location. The most and least noticeable W shapes are for the cheek and back of hand locations, respectively. In fact, the W shape becomes almost a U shape in the case of the back of hand location. At the same time, these W or U

shapes are roughly the same for reflectances measured before and after TWSE at the four body locations. The above-mentioned W shape in skin spectral reflectance factors was reported by Changizi et al. (Changizi, Zhang, & Shimojo, 2006), on the basis of physical models and in connection with hemoglobin variation in human skin. More specifically, these authors indicated that high hemoglobin concentration leads to "a more-defined W feature with a larger difference between its troughs and central peak" and low oxygen saturation in skin hemoglobin leads to a U shape.

It is well known (CIE, 2018) that in the CIELAB space L^* represents lightness, a^* represents red-green, and b^* represents yellow-blue. The associated polar coordinates and perceptual color attributes denominated chroma, C^*_{ab}, and hue-angle, h_{ab}, can also be computed. Let x be any of these CIELAB coordinates, and let $x_{B:j}$ and $x_{A:j}$ represent their values for the j-th participant before (B) and after (A) TWSE, respectively. As skin color appearance is different for different participants, observing the difference between $x_{B:j}$ and $x_{A:j}$ is meaningful. Thus, we will let the paired difference Δx_j be defined by

$$\Delta x_j = x_{A:j} - x_{B:j}, \quad j = 1,2,\cdots,\mathrm{NS} \tag{7}$$

If for a coordinate x, the value before and after TWSE is the same, the paired difference Δx_j, defined by Eq. (7), is 0. Similarly, a positive Δx_j means that the coordinate value after TWSE is higher than before TWSE. The mean, $\overline{\Delta x}$, of the paired differences Δx_j, is

$$\overline{\Delta x} = \frac{1}{NS}\sum_{j=1}^{NS}\Delta x_j = \frac{1}{NS}\sum_{j=1}^{NS}x_{A:j} - \frac{1}{NS}\sum_{j=1}^{NS}x_{B:j} = \bar{x}_A - \bar{x}_B \quad . \tag{8}$$

Figure 4 shows histograms for the paired differences ΔL^* (diagram a), Δa^* (diagram b), Δb^*(diagram c), ΔC^*_{ab} (diagram d), and Δh_{ab} (diagram e) for the four body locations: forehead (top left sub-diagrams), cheek (top right sub-diagrams), neck (bottom left sub-diagrams), and back of hand (bottom right sub-diagrams). M, Med and S are the mean, median and standard deviations of the differences, while the curves are the normal distributions with the means and standard deviations given.

It can be seen from Figure 4 that the mean and median values for ΔL^* and Δh_{ab} are negative for the four body locations, which means that in most cases lightness L^* and hue-angle h_{ab} are lower after TWSE, or exposure of body locations to ultraviolet sunlight radiation. Since $\overline{\Delta L^*} < 0$ and $\overline{\Delta h_{ab}} < 0$, from Eqs. (7) and (8) we have $(\overline{L^*})_A < (\overline{L^*})_B$, and $\left(\overline{h_{ab}}\right)_A < \left(\overline{h_{ab}}\right)_B$ for the four body locations. The result for lightness L^* is as expected, but the result for hue-angle h_{ab}, is new to us.

However, from Figure 4 we can see that the mean and median values for Δa^*, Δb^* and ΔC^*_{ab} are all positives, except Δb^* at the neck position (where mean and median are small, with opposite sign), which means, on the majority, the red-green coordinate a^*, the yellow-blue coordinate b^* and the chroma coordinate C^*_{ab} are higher after TWSE, with the mentioned exception of b^* at neck position. The positive $\overline{\Delta a^*}$, $\overline{\Delta b^*}$ and $\overline{\Delta C^*_{ab}}$ values (see Figure 4) for paired differences (see Eqs. (7) and (8)) imply $(\overline{a^*})_A > (\overline{a^*})_B$, $(\overline{b^*})_A > (\overline{b^*})_B$, and $(\overline{C^*_{ab}})_A > (\overline{C^*_{ab}})_B$ for the four body locations.

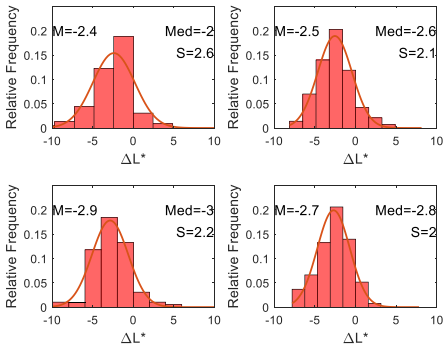

(a)

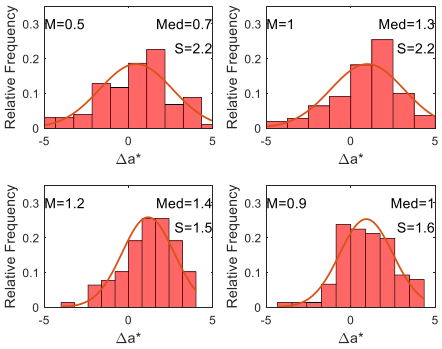

(b)

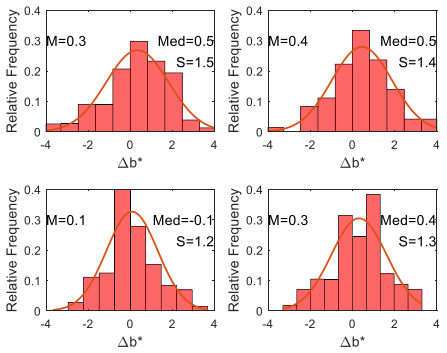

(c)

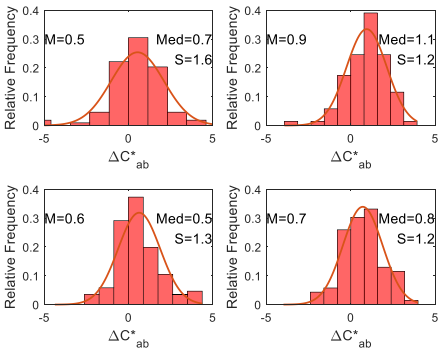

(d)

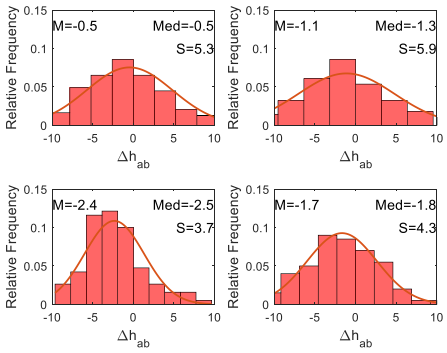

(e)

Figure 4 Histograms for the paired differences ΔL^* (diagram a), Δa^* (diagram b), Δb^*(diagram c), ΔC^*_{ab} (diagram d), and Δh_{ab} [in degrees] (diagram e) at four body locations: forehead (top left sub-diagrams), cheek (top right sub-diagrams), neck (bottom left sub-diagrams), and back of hand (bottom right sub-diagrams). The Δ symbols indicate values after minus values before TWSE (see Eq. (7)). M, Med and S are the mean, median and standard deviations of the differences, respectively, while the curves are the normal distributions with these mean and standard deviations.

From Figure 4, the means in absolute values of the paired differences ($|\overline{\Delta x}|$values) are different for different coordinates and different body locations. The variations (in absolute values) are highest for ΔL^*, lowest for Δb^*, and in between for Δh_{ab}, Δa^*, and ΔC^*_{ab} (from greater to lesser value). Note that Δh_{ab} is shown in a different unit (degree) than the other CIELAB coordinates. These results suggest that L^* may be a good indicator for signaling the variation of melanin concentration, and a^* or C^*_{ab} may also

be better indicators than b^* for the same purpose. Table 2 lists the average CIELAB coordinates before (columns 2-6) and after (columns 7-11) TWSE.

	Before TWSE					After TWSE				
	L^*	a^*	b^*	C^*_{ab}	h_{ab} (°)	L^*	a^*	b^*	C^*_{ab}	h_{ab} (°)
Forehead	55.3	12.2	18.7	22.5	57.0	52.8	12.7	19.1	23	56.5
Cheek	56.6	13.3	17.2	21.8	52.5	54.0	14.2	17.6	22.8	51.3
Neck	55.9	10.8	20.7	23.4	62.7	53.0	11.9	20.8	24.1	60.3
Back of hand	55.5	10.8	19.6	22.4	61.1	52.8	11.8	19.9	23.2	59.5

Table 2 Average CIELAB coordinates before (columns 2-6) and after TWSE (columns 7-11) at the four body locations.

Furthermore, statistical tests were used to find out whether the variations in CIELAB coordinates at different body locations are significant or not. To this aim, the MATLAB *anova1* (one-way ANOVA) was used. The 'test hypothesis' was that the means of $x_{A:j}$ and $x_{B:j}$, for $j = 1,2,\cdots,\mathrm{NS}$ are the same, and the 'alternative hypothesis' was that the means of $x_{A:j}$ and $x_{B:j}$ for $j = 1,2,\cdots,\mathrm{NS}$ are different at 5% significance level. Here again, x is each one of the five CIELAB coordinates, while B and A represent results before and after TWSE. We run the *anova1* software for each of the CIELAB coordinates and each of the four body locations, and p values above/below 0.05 indicate that the test hypothesis must be accepted/rejected. The results found are listed in Table 3.

	L^*	a^*	b^*	C^*_{ab}	h_{ab} (°)
Forehead	Reject	Accept	Accept	Reject	Accept
Cheek	Reject	Reject	Accept	Reject	Accept
Neck	Reject	Reject	Accept	Reject	Reject
Back of hand	Reject	Reject	Accept	Reject	Reject

Table 3 Accept or reject results for the hypothesis of equality of means (0.05 significant level) using the MATLAB *anova1* software, considering each of the 5 CIELAB coordinates and each of the four body locations.

From Table 3, Eqs. (7) and (8), and the means (M) shown in Figure 4, we conclude that the mean lightness $(\overline{L^*})_A$ is significantly lower than the mean lightness $(\overline{L^*})_B$ for any of the four body locations. Hence, for any of the four body locations, skin color appears darker after TWSE, which is consistent with what we observed visually. We can also conclude that the mean red-green coordinate $(\overline{a^*})_A$ is statistically the same as the mean red-green coordinate $(\overline{a^*})_B$ at forehead, while the mean red-green coordinate $(\overline{a^*})_A$ is significantly higher than the mean red-green coordinate $(\overline{a^*})_B$ at cheek, neck and back of hand. Hence, for body locations at cheek, neck and back of hand, skin color appears redder after TWSE. In addition, we can see that the mean yellow-blue coordinate $(\overline{b^*})_A$ is statically the same as the mean yellow-blue coordinate $(\overline{b^*})_B$ for the four body locations though Figure 4(c) shows the differences $(\overline{b^*})_A - (\overline{b^*})_B$ are all positive. Regarding the mean chroma, $(\overline{C^*_{ab}})_A$ is significantly higher than the mean chroma $(\overline{C^*_{ab}})_B$ for any of the four body locations. Hence, for any of the four body locations, skin color appears more colorful after TWSE. Finally, we conclude that the mean hue angle coordinate $(\overline{h_{ab}})_A$ is statistically the same as the mean hue angle coordinate $(\overline{h_{ab}})_B$ at forehead and cheek though Figure 4 (e) shows that the differences $(\overline{h_{ab}})_A - (\overline{h_{ab}})_B$ are negative for these two body locations. However, the mean hue angle coordinate $(\overline{h_{ab}})_A$ is statistically significantly lower than the

mean hue angle coordinate $(\overline{h_{ab}})_B$ for neck and back of hand. From Table 2, all average hue angles h_{ab} are larger than $45°$ and we can say that the percentage of yellowness/redness decreases/increases (CIE, 2018; Li et al., 2017) for the skin appearance after TWSE, specially for the neck and back of hand positions.

4. EVALUATION OF CURRENT DATA USING THE INDIVIDUAL TYPOLOGICAL ANGLE (ITA)

Sunlight irradiation of skin may cause problems such as sunburn, photoaging, pigmentary disorders and cancer. The incidence and extent of these problems is largely related to the skin's degree of constitutive pigmentation. Earlier skin classification was based on self-reporting and interviews (Fitzpatrick, 1988) for clinical treatment. Later, in 1991, Chardon et al. (Chardon, Cretois, & Hourseau, 1991) developed an objective skin classification index, referred to as the individual typological angle (ITA), measured in degrees, which was based on CIELAB coordinates L^* and b^* as follows:

$$\text{ITA} = \frac{180}{\pi} tan^{-1}\left(\frac{L^* - 50}{b^*}\right) \quad . \tag{9}$$

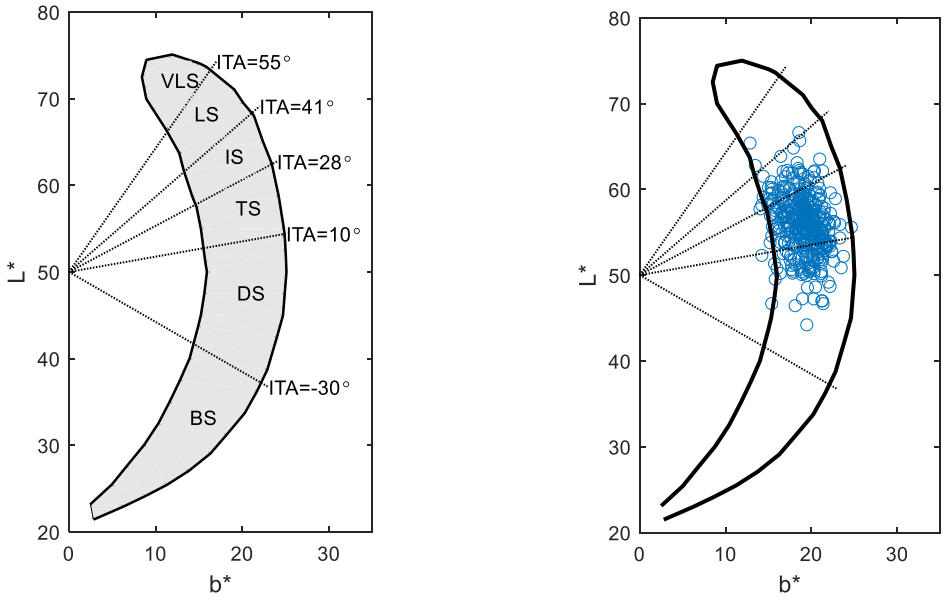

a) b)

Figure 5 a) Constant ITA lines (dotted) separating skin category regions within the shaded area in the CIELAB b^*-L^* plane; b) distribution of current skin colors before TWSE in the CIELAB b^*-L^* plane. The "banana boundary" in a) and b) is based on Figure 1(a) of Del Bino and Bernerd (Del Bino S, & Bernerd F, 2013).

The ITA was developed to establish skin categories such as very light skin (VLS), light skin (LS), intermediate skin (IS), and tan skin (TS), based on average measurements at the lower and upper back for 278 Caucasian volunteers. According to Chardon et al. (Chardon, Cretois, & Hourseau, 1991), L^* values ranged from 53 to 75, a^* values ranged from 2 to 17, and b^* values ranged from 8 to 25. Therefore, the ITA in Eq. (9) was $0°$ when $L^* = 50$, and ITA values were positive for all Caucasian skin colors. From skin reflectance measurements at the cheek for 3,500 women living in France, USA,

Mexico, Brazil, Russia, China, Japan, Thailand and India, Bino and Bernerd (Bino & Bernerd, 2013) confirmed that ITA is correlative with constitutive skin pigmentation and is physiologically relevant in different geographical areas. These authors therefore suggested that ITA could be used for all skin populations, adding the brown skin (BS) and dark skin (DS) categories, as shown in Figure 5a. Chardon et al. (Chardon, Cretois, & Hourseau, 1991) stated that the "a^* coordinate may in the future have to be taken into account", but, to our knowledge, up to now there has been no proposal for ITA modifications incorporating a^*. This point is significant here because, as discussed in Table 3, skin color changes produced by TWSE are more significant for the a^* coordinate than for the b^* coordinate.

In 2001, Zonios et al. (Zonios, Bykowski, & Kollias, 2001) found that ITA and melanin concentration, c_m (in units of x10^{-7} mmole/dl), are linearly correlated, and the larger the ITA is, the lower the c_m. Specifically, from Figure 2 of the paper (Zonios, Bykowski, & Kollias, 2001) by Zonios et al., the next linear formula can be proposed:

$$c_m(\mathrm{x}10^{-7}\ \mathrm{mmole/dl}) = \left(100 - \left(\frac{100}{48}\right)\mathrm{ITA}\right) \quad . \tag{10}$$

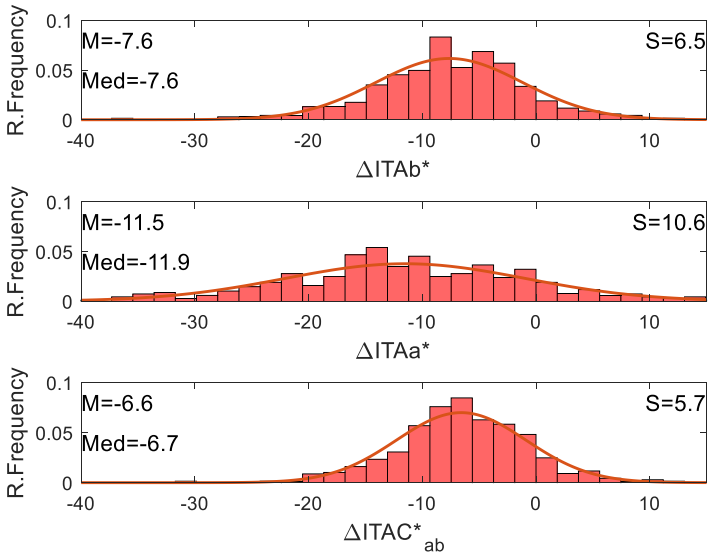

Figure 6 Histograms for paired differences $\Delta\mathrm{ITA}b^*$ (top diagram), $\Delta\mathrm{ITA}a^*$ (middle diagram), and $\Delta\mathrm{ITA}C^*_{ab}$ (bottom diagram), where all Δ's mean values after TWSE minus values before TWSE. M, Med and S are the mean, median and standard deviations of the paired differences and the plotted curves are the normal distributions with these means and standard deviations.

Analysis of the data gathered in the previous section reveals important differences in skin color appearance before and after TWSE, which can be considered a consequence of natural sunlight tanning. Hence, our current data have also been used to evaluate ITA, our expectation being that ITA decreases as a consequence of TWSE. However, from Table 3 in the previous section, the a^* and C^*_{ab} coordinates may serve better than b^* to show the variation in skin color appearance produced by TWSE. Therefore, in addition to the ITA index defined in Eq. (9) using L^* and b^* (a combination henceforth referred to as $\mathrm{ITA}b^*$ in this paper), two analogous indices are now proposed, using L^* and a^* (named $\mathrm{ITA}a^*$), and L^* and C^*_{ab} (named $\mathrm{ITA}C^*_{ab}$). To compare $\mathrm{ITA}b^*$, $\mathrm{ITA}a^*$, and $\mathrm{ITA}C^*_{ab}$ using our current data, we can disregard body location and put together all data shown in Table 1. As in the previous section, we also consider the paired differences:

$$\Delta\mathrm{ITA}x_j = \mathrm{ITA}x_{A:j} - \mathrm{ITA}x_{B:j}, \quad j = 1,2,\cdots,\mathrm{N} \tag{11}$$

where, x can be b^*, a^*, and C^*_{ab}, the sub-indices B and A mean before and after TWSE, respectively, and $\mathrm{N} = 367$. Figure 6 shows histograms (Relative (R.) Frequency) for the paired differences $\Delta\mathrm{ITA}b^*$ (top diagram), $\Delta\mathrm{ITA}a^*$ (middle diagram), and $\Delta\mathrm{ITA}C^*_{ab}$ (bottom diagram), respectively. In Figure 6, M, Med and S are the mean, median and standard deviations of the paired differences, and the plotted curves are the normal distributions with the given means and standard deviations. It can be seen from Figure 6 that mean and median values are all negative for $\Delta\mathrm{ITA}b^*$ (top diagram), $\Delta\mathrm{ITA}a^*$ (middle diagram), and $\Delta\mathrm{ITA}C^*_{ab}$ (bottom diagram). Hence in most cases we have $\Delta\mathrm{ITA}x_j < 0$ (see Eq. (11)), which means that, on the whole, $\mathrm{ITA}x_{A,j} < \mathrm{ITA}x_{B,j}$, as expected.

In order to determine which of the three indices, $\mathrm{ITA}b^*$, $\mathrm{ITA}a^*$, or $\mathrm{ITA}C^*_{ab}$, is more appropriate, we used the L^* coordinate as reference, because it was the one with the greatest change during TWSE (see Figure 4 and Table 3). First, we separated our data into two groups: Group 1 when $L^*_{B,j} > L^*_{A,j}$, and Group 2 when $L^*_{B,j} \leq L^*_{A,j}$. Thus, for the data in Group 1 we can expect $(\mathrm{ITA}x)_{B,j} > (\mathrm{ITA}x)_{A,j}$, and therefore obtaining $(\mathrm{ITA}x)_{B,j} \leq (\mathrm{ITA}x)_{A,j}$ (i.e. the opposite result) can be considered a "wrong decision" (WD). Analogously, for the data in Group 2, $(\mathrm{ITA}x)_{B,j} > (\mathrm{ITA}x)_{A,j}$ may also be considered a "wrong decision" (WD). Table 4 shows the "number of wrong decisions" (NWDs) using $\mathrm{ITA}b^*$, $\mathrm{ITA}a^*$ and $\mathrm{ITA}C^*_{ab}$. From Table 4, $\mathrm{ITA}C^*_{ab}$ is the best index, because it achieves the lowest NWDs, followed by $\mathrm{ITA}b^*$ and $\mathrm{ITA}a^*$. Besides this, a^* was a better indicator than b^* for quantifying skin color variation due to TWSE, as discussed in the previous section (see Table 3). The great improvement of $\mathrm{ITA}C^*_{ab}$ with respect to $\mathrm{ITA}b^*$ and $\mathrm{ITA}a^*$ indicates that using only one of the two coordinates b^* and a^* is not enough, and both can be incorporated to improve results, using the new $\mathrm{ITA}C^*_{ab}$ index.

	$\mathrm{ITA}b^*$	$\mathrm{ITA}a^*$	$\mathrm{ITA}C^*_{ab}$
NWDs	9	15	4

Table 4 Number of wrong decisions (NWDs) using $\mathrm{ITA}b^*$, $\mathrm{ITA}a^*$, and $\mathrm{ITA}C^*_{ab}$ at the four body locations for the whole TWSE dataset, when the measured lightness L^* is considered as reference.

Furthermore, during TWSE the skin of every participant was continuously exposed to natural sunlight irradiation. Therefore, finally, we can expect that the increase of melanin concentration in skin (Δc_m) will be nearly the same for all of them, assuming that response to ultraviolet radiation is the same for all participants. Thus, from Eqs. (10) and (11), we may expect $\Delta\mathrm{ITA}x$ to be the same for all. This is not the case, however, and $\Delta\mathrm{ITA}x$ is distributed normally, as shown in Figure 6. In any case, we can note that $\Delta\mathrm{ITA}a^*$ has the greatest standard deviation, $\Delta\mathrm{ITA}C^*_{ab}$ the lowest, and $\Delta\mathrm{ITA}b^*$ is in between. Therefore, $\mathrm{ITA}C^*_{ab}$ with the lowest standard deviation (S=5.7) can be considered as the best result, $\mathrm{ITA}b^*$ the second best, and $\mathrm{ITA}a^*$ the worst. This result is consistent with the order of performance we found using NWDs, with L^* as reference (Table 4).

Note that recently Zhao et al. (Zhao et al., 2017) also considered ITA for predicting skin whiteness. They developed a new $\mathrm{ITA}C^*_{ab}$ index using the L^* and C^*_{ab} coordinates, replacing 50 by 40.28 in the previous Eq. (9). They also found that their new $\mathrm{ITA}C^*_{ab}$ was better than $\mathrm{ITA}b^*$ for predicting skin whiteness.

5. CONFIDENCE ELLIPSES ASSOCIATED TO ITA SKIN CATEGORIES

In the evaluation of cosmetic sun products, it is usual to consider the skin categories established by the ITA index (Chardon, Cretois, & Hourseau, 1991), and to examine the suntan effect and color shifts for different skin types exposed to solar simulators in the laboratory. Normally, the number of volunteers for this kind of research is relatively low. For example, 14 volunteers participated in the experiment of Chardon et al. (Chardon, Cretois, & Hourseau, 1991), and 10 participated in the experiment of Zonios et al. (Zonios, Bykowski, & Kollias, 2001). Recently, Amano et al. (Amano et al., 2020) applied sunless tanning products (dihydroxyacetone -DHA- gels) to volunteers, and examined the naturalness of color shifts, for an experimental and a control group, using the CIELAB color space. The control group had 60 Caucasian volunteers, whose skin colors were measured at the inner and outer forearm positions, and the difference between these two positions was assumed to be caused by natural sunlight irradiation.

To complement earlier studies, we have analyzed the skin color shifts in the CIELAB space using our current data on the effect of TWSE (designated as MT dataset), comparing with the data from the control group (designated as CG dataset) in Amano et al. paper (Amano et al., 2020). The amount of color data in the skin categories established by the ITA index for the MT and CG datasets are listed in Table 5. As indicated in Table 1, after removing outliers the MT dataset had 367 skin colors, which were plotted in Fig. 5b for measurements before TWSE, while the CG dataset had 60 skin colors.

	Skin Category				
Dataset	VLS	LS	IS	TS	DS
MT	0	3	**52**	**220**	**92**
CG	**24**	**25**	**10**	1	0

Table 5 Amount of data in each of the 5 ITA skin categories, for the current TWSE (MT) dataset and the control group (CG) dataset in Amano et al., 2020 study.

Traditionally, ellipses and ellipsoids have been used in color science to describe different kind of color variations (MacAdam, 1942; Melgosa et al., 1994). In the current section, we will analyze the main parameters of ellipses obtained from the MT and CG datasets in different CIELAB planes, considering different skin categories defined by the ITA index, as well as parameters of the straight line joining the centers of two "related ellipses". By "related ellipses" we mean two ellipses in the same ITA category, one from data before TWSE and the other for data after TWSE, in the case of the MT dataset, or one from data in the inner forearm and the other from data in the outer forearm, in the case of the CG dataset. In the next analyses we omitted those skin categories with fewer than 10 colors, indicated with non-bold numbers in Table 5, fitting 95% confidence ellipses (Amano et al., 2020) to the measured data for each of the remaining skin categories. Figure 7 shows the color shifts in the b^*-L^* plane using the MT (a) and CG (b) datasets for the VLS (magenta), LS (red), IS (blue), TS (black), and DS (cyan) skin categories defined by the ITA index. The same colored solid/dotted ellipses with their centers indicated by solid circles/stars correspond to data measured before/after TWSE (Fig. 7a) and data measured at the inner/outer forearm (Fig 7b). For each dataset (MT and CG) and skin type (ITA index), Table 6 shows different parameters of the ellipses fitted in the b^*-L^* plane: Coordinates of ellipses centers, lengths of the major (Ma) and minor (Mi) axes, orientation of the major axis (in degrees) relative to the horizontal axis, distances (D) and slopes (SL) of the straight line joining "related ellipses".

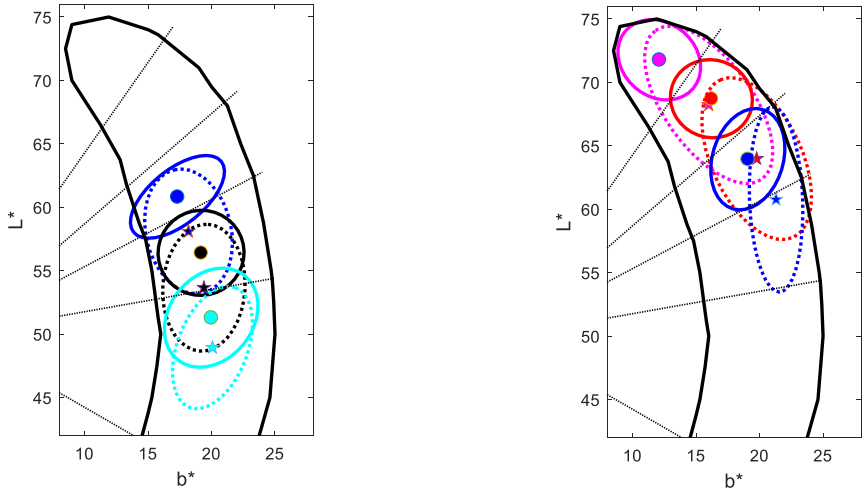

a) MT b) CG (Amano et al., 2020)

Figure 7 Color variations in the b^*-L^* plane using the MT (a) and CG (b) datasets for the ITA skin categories VLS (magenta), LS (red), IS (blue), TS (black), and DS (cyan). Solid/dotted ellipses with their respective centers indicated by solid circles/stars represent results from measured data before/after TWSE in plot a), and measured data at the inner/outer forearm (Amano et al., 2020) in plot b).

Dataset	Skin type (ITA)	Mode	Center's abscissa	Center's ordinate	Major axis Ma	Minor axis Mi	Major axis Orient. (°)	D	SL
MT	IS	Before	17.3	60.8	4.4	2.2	39	2.9	-3.1
		After	18.2	58.1	5	3.4	-77		
	TS	Before	19.2	56.4	3.4	3.3	-21	2.8	-12.2
		After	19.4	53.7	5	3.2	-86		
	DS	Before	20	51.3	4.2	3.3	52	2.4	-22.4
		After	20.1	48.9	5.1	2.8	69		
CG	VLS	Inner	12.1	71.8	3.5	2.9	-41	5.3	-0.9
		Outer	16	68.2	7.2	3.5	-55		
	LS	Inner	16.2	68.7	3.3	3.1	-20	5.9	-1.3
		Outer	19.8	64	6.8	3.6	-65		
	IS	Inner	19.1	63.9	4.1	2.8	73	3.9	-1.4
		Outer	21.3	60.8	7.3	2.1	-88		

Table 6 Main parameters of ellipses plotted in Fig. 7 (plane b^*-L^*, MT and CG datasets, different skin types): Centers' abscissa and ordinate, lengths of Major (Ma) and Minors (Mi) axes, orientation of the major axes (in degrees) relative to the horizontal axis, distances (D) and slopes (SL) of the straight line joining related ellipses centers.

Results in Table 6 for the MT and CG datasets can be compared, bearing in mind that both correspond to natural suntanning effects. First, we can see that the major axis increases after the TWSE for each of the skin categories for the MT dataset. Roughly, this increase in magnitude of the major axes is in the range from 0.6 to 1.6. For the CG dataset, the major axis also increases for the outer forearm position compared with the inner forearm position for each of the skin categories, but this increase is in the range from 3 to 4, which is much higher than the one for the MT dataset. Regarding length of minor axes, it increases for the IS category and decreases for the TS and DS categories after the TWSE, and

decreases for the IS category and increases for the VLS and LS categories in the CG dataset. From Table 6 we can also see that color shifts (D) for the MT dataset are smaller and with higher slopes (SL) than for the CG dataset (see also Figs. 7a-7b). These discrepancies may be attributed to two facts: 1) Differences in skin irradiation times (only two weeks for the MT dataset vs. a much longer period for the CG dataset); 2) Consideration of different skin locations (for the MT dataset we measured at the same skin locations, but for the CG dataset measurements were made at two different skin locations, perhaps with different skin chromophores (Young, 1997)).

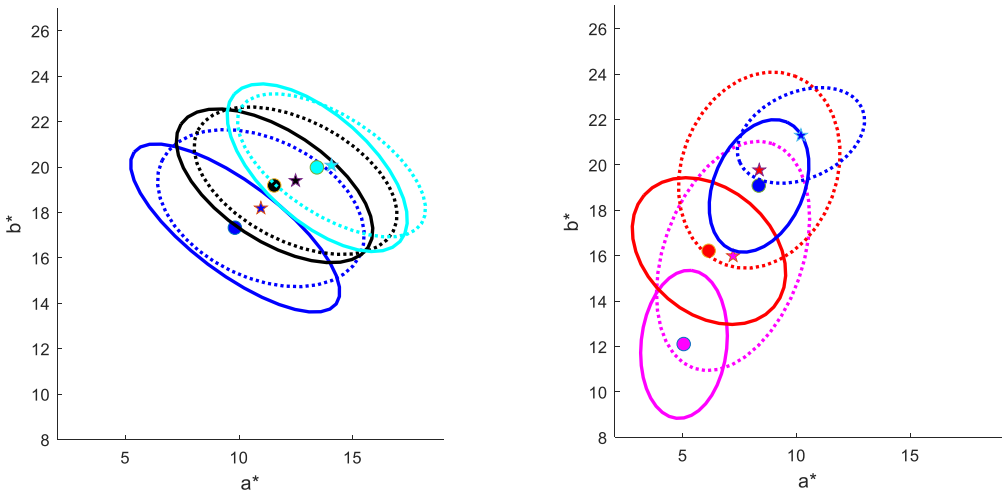

a) MT

b) CG (Amano et al., 2020)

Figure 8 Idem to Fig. 7, except for the a^*-b^* plane.

Dataset	Skin type (ITA)	Mode	Center's abscissa	Center's ordinate	Major axis Ma	Minor axis Mi	Major axis Orient. (°)	D	SL
MT	IS	Before	9.8	17.3	5.6	2	-37	1.4	0.8
		After	11	18.2	4.8	3.1	-26		
	TS	Before	11.6	19.2	4.9	2.4	-34	1.0	0.2
		After	12.5	19.4	4.8	2.7	-27		
	DS	Before	13.4	20	4.9	2.4	-42	0.6	0.2
		After	14.1	20.1	4.7	2.2	-33		
CG	VLS	Inner	5	12.1	3.3	1.9	84	4.5	1.8
		Outer	7.2	16	5.2	3.1	71		
	LS	Inner	6.1	16.2	3.8	2.8	-41	4.2	1.6
		Outer	8.4	19.8	4.4	3.4	70		
	IS	Inner	8.4	19.1	3.1	2	66	2.9	1.2
		Outer	10.2	21.3	2.9	1.9	24		

Table 7 Idem to Table 6, except for the a^*-b^* plane.

Figure 8 shows fitted ellipses in the a^*-b^* plane using the same two datasets. All colors and symbols of ellipses in Figure 8 have the same meanings as those in Figure 7. Similar to Table 6 for the b^*-L^* plane, Table 7 lists the ellipses and color shifts parameters in the a^*-b^* plane. From Table 7 we can see that the distances (D) and slopes (SL) for the MT dataset are smaller than those for the CG

dataset, as in Table 6. In addition, Table 7 shows that the major axis decreases for each of the skin categories after the TWSE, but for the CG dataset it decreases for the IS category and increases for the VLS and LS categories. As for the minor axis, results in Table 7 indicate that it increases for the IS and TS categories and decreases for the DS category after the TWSE, while it decreases for the IS category and increases for the VLS and LS categories for the CG dataset. It can be assumed that the reasons of the disagreements between MT and CG datasets are the same stated in the previous paragraph.

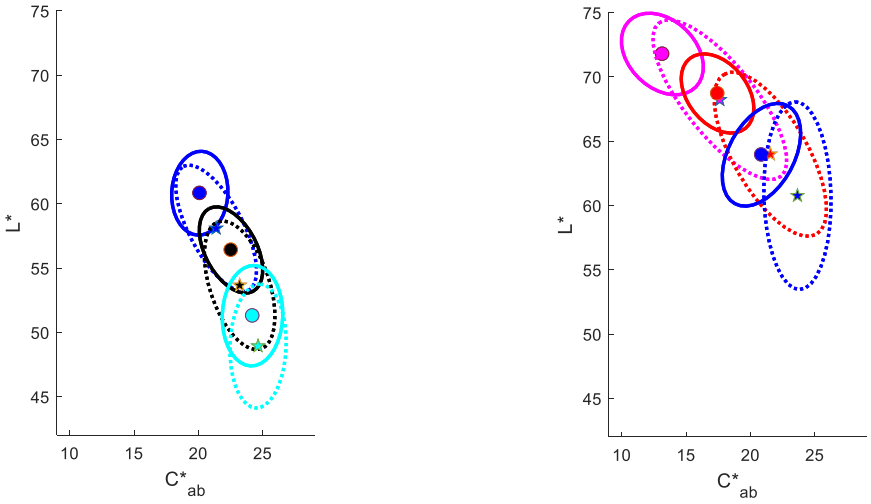

a) MT

b) CG (Amano et al., 2020)

Figure 9 Idem to Fig. 7, except for the C^*_{ab}-L^* plane.

Dataset	Skin type (ITA)	Mode	Center's abscissa	Center's ordinate	Major axis Ma	Minor axis Mi	Major axis Orient. (°)	D	SL
MT	IS	Before	20.1	60.8	3.3	2.2	87	3	-2.1
		After	21.4	58.1	5.4	2.1	-62		
	TS	Before	22.5	56.4	3.6	2	-62	2.8	-4.1
		After	23.2	53.7	5.2	2.3	-72		
	DS	Before	24.2	51.3	3.9	2.3	88	2.4	-5.4
		After	24.6	48.9	4.8	2.2	88		
CG	VLS	Inner	13.1	71.8	3.6	2.6	-45	5.7	-0.8
		Outer	17.6	68.2	7.6	2.7	-52		
	LS	Inner	17.4	68.7	3.5	2.3	-52	6.3	-1.2
		Outer	21.5	64	7.2	2.9	-60		
	IS	Inner	20.8	63.9	4.3	2.6	62	4.2	-1.1
		Outer	23.6	60.8	7.3	2.6	-89		

Table 8 Idem to Table 6, except for the C^*_{ab}-L^* plane.

Figure 9 shows fitted ellipses in the C^*_{ab}-L^* plane for the two datasets under study. All colors and symbols of ellipses in Figure 9 have the same meaning as those in previous Figures 7 and 8. As in previous Tables 6 and 7, Table 8 lists the values of the ellipses parameters and color shifts in the C^*_{ab}-L^* plane. From Table 8 the distances (D) and slopes (SL) for MT are again lower than for CG. As for the major axes, Table 8 shows that they increase for all skin categories after the TWSE, and also increase for the outer forearm position compared with respect to the inner forearm position in the CG dataset.

However, the increase of length of the major axis is much higher for the CG dataset than for the MT dataset. Regarding the minor axes, Table 8 indicate that they slightly decrease for the IS and DS categories and increase for the TS category after the TWSE, while for the CG dataset they are almost constant, except for the LS category where there is an increase.

In overall, we can say that "related ellipses" from MT and CG datasets are different. While both datasets may be considered as results of natural suntanning, they also have differences regarding the irradiation times and measured body locations, which may partly explain this result.

6. CONCLUSIONS

Using a CM-2600d spectrophotometer we performed skin color measurements at four different body locations, before and after TWSE. From 103 participants, a total of 3,296 skin spectra were measured. The repeatability of our measurements before and after TWSE at the four body locations ranged from 0.2 to 0.5 CIELAB units. However, skin color variations produced by TWSE was above 3.6 CIELAB units for all of the four body locations measured, which is significantly higher than repeatability, and also greater than the 0.6-1.1 CIELAB units, reported as a typical range of magnitude for the visual color thresholds of subjects with normal color vision (Huang et al., 2015).

Changizi et al. (Changizi, Zhang, & Shimojo, 2006) used a physical model and reported that skin spectral reflectances have a clear W shape between 520 nm and 600 nm, with variations depending on hemoglobin concentration and oxygen saturation. Our current measurements showed this W shape (Figure 3), with variations depending on the measured body location. In particular, we found that the W shape is most noticeable at the cheek location and least noticeable at the back of hand location, where in fact the W shape becomes almost a U shape. At the same time, we found that the W or U shapes were roughly the same for reflectances measured before and after TWSE at all of the four body locations measured.

Analyses in the CIELAB color space showed that TWSE made the L^* and h_{ab} coordinates significantly decrease, except at the forehead and cheek positions for the h_{ab} coordinate. Even with these exceptions, after TWSE the h_{ab} coordinate decreased on average 0.5° and 1.3° for forehead and cheek, respectively, which are not, however, statistically significant changes. The L^* change produced by TWSE was greater than 2.4 units (see M values in Figure 4) for any of the four body locations, which clearly indicates that the skin appears darker after TWSE. This is consistent with visual observations. The decrease in h_{ab} produced by TWSE indicates an increase in the percentage of redness and a decrease in the percentage of yellowness in hue composition, particularly for the neck and back of hand locations. With regard to a^* and C^*_{ab}, it was found that they significantly increased as a consequence of TWSE for all four body locations, except in the case of the a^* coordinate at forehead. For b^* coordinate it was found that there was no significant variation produced by TWSE for any of the four body locations. The highest average variations produced by TWSE were for the L^* coordinate, followed by h_{ab} a^*, C^*_{ab}, and b^*, in that order. Note that h_{ab} is measured in degrees, a different unit than the ones for all other CIELAB coordinates.

From our measured data we evaluated the ITA index (Chardon, Cretois, & Hourseau, 1991) and proposed two modifications. According to the number of "wrong decisions" using L^* as reference, and considering the distributions of the $\Delta\mathrm{ITA}x$ indices, it was found that $\mathrm{ITA}C^*_{ab}$ is the best index, followed by $\mathrm{ITA}b^*$ (Chardon, Cretois, & Hourseau, 1991) and $\mathrm{ITA}a^*$, in that order, although a^* was found to be a better indicator than b^* for quantifying the variations produced by TWSE.

Finally, we studied color shifts in different planes formed by combinations of CIELAB coordinates, according to the different skin categories established by ITAb^* (Chardon, Cretois, & Hourseau, 1991), and compared our current results with the ones in the control group from Amano et al. (Amano et al., 2020). We used 95% confidence ellipses to present data distributions in the planes concerned for each of the VLS, LS, IS, TS, and DS skin categories. The distances and slopes between the centers of "related ellipses" were also analyzed, and it was found that the distances and slopes for TWSE data are different from those in the Amano et al. control group (Amano et al., 2020), while both datasets may be considered as results of natural suntanning. Our current data plus the control group data in Amano et al., 2020 may be useful for future comparisons made with data obtained from using new sunless tan products or sun protection products. In this respect, it must be considered that in Western countries the white population considers suntanning to be healthy and socially attractive, while in Asia most people prefer lighter skin colors.

The skin spectra measured in this paper constitute additions to the CIE TC 1-92 skin color database, complementing those currently being gathered. Current skin spectra can also be considered as representative of natural suntanning processes, and can be compared with data reported in the literature, usually obtained in the laboratory by using solar simulators. It is also expected that the data and results in this paper will find applications in the fields of computer graphics, digital animation, and film production.

ACKNOWLEDGEMENTS

The authors thank Kinjiro Amano and Sophie Wuerger for sharing their data with us for this research. English assistance from Mr. Donald J. Murphy McVeigh is acknowledged. This study was supported by the National Natural Science Foundation of China [grant numbers 61575090, 61775169]; the Ministry of Science and Innovation of the Government of Spain [Project PID2019-107816GB-I00 funded by MCIN/AEI/10.13039/501100011033]; the Natural Science Foundation of Liaoning Province [grant number 2019-ZD-0267]; and the Foundation of Liaoning Province Education Administration [grant number 2020LNJC01, LJKZ0319].

ORCID

Changjun Li https://orcid.org/0000-0002-9942-7690

Manuel Melgosa https://orcid.org/0000-0002-7226-4190

Data Availability Statement

The data used to support the findings of this study are available from the corresponding author upon request. The data are not publicly available due to privacy restrictions.

REFERENCES

Amano, K., Xiao, K., Wuerger, S., & Meyer, G. (2020). A colorimetric comparison of sunless with natural skin tan. *PLoS ONE*. 15(12), e0233816. https://doi.org/10.1101/2020.05.14.095778

Bilal, S., Akmeliawati, R., Salami, M. J. E., & Shafie, A. A. (2015). Dynamic approach for real-time skin detection. *J. Real Time Image Process*. 10, 371–385. https://doi.org/10.1007/s11554-012-0305-2

Bino, S.D., & Bernerd, F. (2013). Variations in skin colour and the biological consequences of ultraviolet radiation exposure. *British Journal of Dermatology*. 169(s3), 33–40. https://doi.org/10.1111/bjd.12529

Brancati, N., Frucci, M. D., Pietro, G., & Gallo, L. (2016). Dynamic clustering for skin detection in YCBCR colour space. Pattern Recogn. Inform. Process, 49–53. http://elib.bsu.by/handle/123456789/158528

Chardon, A., Cretois, I., & Hourseau, C. (1991). Skin colour typology and suntanning pathways. *Int. J. Cosmetic Sci*. 13, 191-208. https://doi.org/10.1111/j.1467-2494.1991.tb00561.x

Changizi, M. A., Zhang, Q., & Shimojo, S. (2006). Bare skin, blood and the evolution of primate colour vision. *Biol. Lett*. 2(2), 217-221. https://doi.org/10.1098/rsbl.2006.0440

CIE Publication 015:2018 (2018). Colorimetry, 4th edition. CIE Central Bureau, Vienna. https://doi.org/10.25039/TR.015.2018

Durand, C., Catelinois, O., Bord, A., Richard, J. B., Bidondo, M. L., Menard, C., Cousson-Gelie, F., Mahe, E., Mouly, D., & Delpierre C. (2020). Effect of an appearance-based vs. a health-based sun-protective intervention on French summer tourists' behaviors in a cluster randomized crossover trial: The PRISME protocol. *Frontiers in Public Health*. 8, 569857. https://doi.org/10.3389/fpubh.2020.569857

Fairchild, M.D. (2013). Color Appearance Models, 3rd Edition. Wiley, New York.

Fitzpatrick, T. B. (1988). The validity and practicality of sun-reactive skin types I through VI. *Arch. Dermatol*. 124(6), 869-871. https://doi.org/10.1001/archderm.1988.01670060015008

Han, K., Choi, T., & Son, D. (2006). Skin color of Koreans: statistical evaluation of affecting factors. *Skin Research and Technology*. 12(3), 170-177. https://doi.org/10.1002/col.22679

Huang, M., Cui, G., Melgosa, M., Sánchez-Marañón, M., Li, C. J., Luo, M. R., & Liu, H. (2015). Power functions improving the performance of color-difference formulas. *Opt. Express.* 23(1), 597-610. https://doi.org/10.1364/OE.23.000597

Konica Minolta. Spectrophotometer CM-2600d/2500d, Instruction Manual. https://www.konicaminolta.com/instruments/download/instruction_manual/color/pdf/cm-2600d-2500d_instruction_eng.pdf

Jiang, L., Wang, H., Zhang, H., Gao, C., Xiao, K., Melgosa, M., & Li, C. (2021). Characterizing skin color before and after 100-m sprinting. *Color Res Appl*. 1–10. https://doi.org/10.1002/col.22679

Li, C. J., Li, Z., Wang, Z., Xu, Y., Luo, M. R., Cui, G., Melgosa, M., Brill, M. H., & Pointer, M. (2017). Comprehensive colour solutions: CAM16, CAT16 and CAM16-UCS. *Color Res. Appl*. 42, 703–718. https://doi.org/10.1002/col.22131

MacAdam, D. L. (1942). Visual sensitivities to color differences in daylight. *J. Opt. Soc. Am.* 32(5), 247-274. https://doi.org/10.1364/JOSA.32.000247

Melgosa, M., Hita E., Romero, J., Jimenez del Barco, L. (1994). Color-discrimination thresholds translated from the CIE (*x,y,Y*) space to the CIE 1976 (*L*,a*,b**). *Color Res. Appl.* 19(1), 10-18. https://doi.org/10.1111/j.1520-6378.1994.tb00054.x

Melgosa, M, Pérez, M.M., Moraghi A. El, Hita E. (1999). Color discrimination results from a CRT device: Influence of luminance. *Color Res. Appl.* 24(1), 38-44. https://doi.org/10.1002/(SICI)1520-6378(199902)24:1<38::AID-COL8>3.0.CO;2-I

Melgosa, M., Richard, N., Fernández-Maloigne, C., Xiao, K., de, Clermont-Gallerande, H., Jost-Boissard, S., & Okajima, K. (2018). Colour differences in Caucasian and Oriental women's faces illuminated by white light-emitting diode sources. *Int. J. Cosmetic Sci*. 40, 244-255. https://doi.org/10.1111/ics.12457

Melgosa M., Rivas M.J., Hita E., Vièmot F. (2000). Are we able to distinguish color attributes? *Color Res. Appl.* 25(5), 356-367. https://doi.org/10.1002/1520-6378(200010)25:5<356::AID-COL6>3.0.CO;2-S

Mendenhall, M. J. , Nunez, A. S., & Martin, R. K. (2015). Human skin detection in the visible and near infrared. *Appl. Opt*. 54(35), 10559-10570. https://doi.org/10.1364/AO.54.010559

Schmitt, J. M., & Kumar, G. (1996). Turbulent nature of refractive-index variations in biological tissue. *Opt. Lett*. 21, 1310-1312. https://doi.org/10.1364/OL.21.001310

Wang, Y., Luo, M. R., Wang, M., Xiao, K., & Pointer, M. (2018). Spectrophotometric measurement of human skin colour. *Color Res. Appl*. 43(4), 458–470. https://doi.org/10.1002/col.22143

Wei, L., Xuemin, W., Wei, L., Li, L., Ping, Z., Yanyu, W., Ying, L., Yan, L., Yan, T., & Yan, W. (2007). Skin color measurement in Chinese female population: analysis of 407 cases from 4 major cities of China. *Int. J. Dermatol*. 46(8), 835-839. https://doi.org/10.1111/j.1365-4632.2007.03192.x

Xiao, K., Liao, N., Zardawi, F., Liu, H., Noort, R. V., Yang, Z., Min, H., & Yates, J. M. (2012). Investigation of Chinese skin colour and appearance for skin colour reproduction. *Chinese Opt*. 10(008), 74-78. https://doi.org/10.3788/COL201210.083301

Xiao, K., Yates, J. M., Zardawi, F., Sueeprasan, S., Liao, N., Gill, L., Li, C., & Wuerger, S. (2017). Characterising the variations in ethnic skin colours: a new calibrated data base for human skin. *Skin Research and Technology*. 23(1), 21-29. https://doi.org/10.1111/srt.12295

Xiao, K., Zardawi, F., Van, Noort, R., & Yates, J. M. (2013). Color reproduction for advanced manufacture of soft tissue prostheses. *J. Dent*. 41(Suppl. 5), e15–e23. https://doi.org/10.1016/j.jdent.2013.04.008

Xiao, K., Zhu, Y., Li, C. J., Connah, D., Yates, J. M., & Wuerger, S. (2016). Improved method for skin reflectance reconstruction from camera images. *Opt. Express*. 24(13), 14934-14950. https://doi.org/10.1364/OE.24.014934

Young, A.R. (1997). Chromophores in human skin. *Phys. Med. Biol*. 42, 789-802. https://doi.org/10.1088/0031-9155/42/5/004

Zhang, H.Q., Montag, E. D. (2006). How well can people use different color attributes? *Color Res. Appl*. 31(6), 445-457. https://doi.org/10.1002/col.20257

Zhao, B., Pan, Q., Wang, Z., Xu, Y., Li, C., Westland, S., & Xiao, K. (2017). Developing a model for predicting whiteness of human face, in proceedings of 13TH AIC CONGRESS (AIC 2017), BEING COLOR WITH HEALTH, 16th-20th, October, 2017, JEJU, KOREA. OS09-04.

Zonios, G., Bykowski, J., & Kollias, N. (2001). Skin melanin, hemoglobin, and light scattering properties can be quantitatively assessed in vivo using diffuse spectroscopy. *J. Invest. Dermatol*. 117(6), 1452-1457. https://doi.org/10.1046/j.0022-202x.2001.01577.x

Zonios, G., Perelman, L. T., Backman, V., Manoharan, R., & Feld, M. S. (1999). Diffuse reflectance spectroscopy of human adenomatous colon polyps in vivo. *Appl. Opt*. 38(31), 6628-6637. https://doi.org/10.1364/AO.38.006628